

Cite this: DOI: 00.0000/xxxxxxxxxx

## Yield stress "in a flash": investigation of nonlinearity and yielding in soft materials with an optofluidic microrheometer<sup>†</sup>

Valerio Vitali,<sup>a\*</sup> Giovanni Nava,<sup>b</sup> Andrea Corno,<sup>b</sup> Melissa Pezzotti,<sup>a</sup> Francesca Bragheri,<sup>c</sup> Petra Paiè,<sup>c</sup> Roberto Osellame,<sup>c,d</sup> Marco Aldo Ortenzi,<sup>e</sup> Ilaria Cristiani,<sup>a</sup> Paolo Minzioni,<sup>a</sup> Tommaso Bellini,<sup>b</sup> and Giuliano Zanchetta<sup>b\*\*</sup>

### Supplementary Information

#### Microrheometer calibration

The microrheometer calibration was carried out by performing optical shooting experiments in Newtonian fluids of known viscosity  $\eta$ , such as water. The raw data acquired from the tracking of the microbead position during the optical shooting procedure are space-time trajectories  $x(t)$ . Due to the low Reynolds number, it is possible to neglect the inertial effects during the movement of the microbead inside the microfluidic channel. Therefore, considering a microsphere with radius  $R$  in a Newtonian fluid, it can be reasonably assumed that the optical scattering force  $F_o$  exerted by the impinging laser beam will be equal to the Stokes drag force in each position and instant of time during the bead movement:

$$F_o(x, P_L) = 6\pi R\eta \frac{dx}{dt} \quad (\text{S1})$$

where  $P_L$  is the optical power emitted by the laser source. Since the optical force depends on the microbead position  $x$ , but not on the time instant  $t$ , it is possible to separate the two variables and obtain the following equation:

$$\int_{t_i}^{t^* < t_f} dt = \int_{x_i}^{x^* < x_f} \frac{6\pi R\eta}{F_o(x, P_L)} dx \quad (\text{S2})$$

where  $(t_i, x_i)$  and  $(t_f, x_f)$  represent the initial and final coordi-

nates of the microbead trajectory, while  $(t^*, x^*)$  represent the coordinates at a generic instant of the shooting experiment. The optical force can be rewritten as  $F_o = AP_L f(x)$ , where  $A$  is the calibration constant to be determined,  $P_L$  is the optical power emitted by the laser source, which is known, and  $f(x)$  is the optical force profile, which can be precisely calculated by means of numerical simulations based on paraxial ray-optics (PRO) approach<sup>1,2</sup>. In order to determine the calibration constant  $A$ , it is possible to define the following function, based on Eq. S2:

$$R(t^*) = \int_{t_i}^{t^* < t_f} dt - \frac{6\pi R\eta}{AP_L} \int_{x_i}^{x^* < x_f} \frac{dx}{f(x)} \quad (\text{S3})$$

The value of the calibration constant  $A$  can be determined by performing optical shooting experiments in fluids of known viscosity (such as milliQ water) and by minimizing the value of  $\int_{t_i}^{t_f} R(t^*)^2 dt^*$ . The calibration procedure was carried out before and after each measurement campaign to verify the system stability in terms of applied optical force. The difference between the value of the calibration constant measured before and after each experimental session was always found to be lower than 2%, confirming the good system stability, which can be attributed to the high level of integration between microfluidic and optical components in the chip.

#### Optical force profiles for PS and TBG microbeads

As previously discussed, the stress acting on the microbead can be written as  $\sigma = F_o/(12\pi R^2)$ , where  $F_o = AP_L f(x)$  is the optical force acting on the microbead. The optical force profile  $f(x)$  describes the dependence of the optical force on the microbead position along the microchannel and depends on different parameters, such as the wavelength and beam waist of the laser beam emitted by the waveguide, the microbead radius and the refractive index of the fluid and microbead. Notably, it is possible to achieve large optical forces by increasing the refractive index contrast between the medium and the microbead used as tracer. As discussed in the main text, we employed polystyrene (PS) microbeads (Sigma Aldrich 72986, radius  $R = 5 \mu\text{m}$ , re-

<sup>a</sup>Dipartimento di Ingegneria Industriale e dell'Informazione, Università di Pavia, 27100 Pavia, Italy

<sup>b</sup>Dipartimento di Biotecnologie Mediche e Medicina Traslazionale, Università di Milano, 20090 Segrate (MI), Italy. E-mail: giuliano.zanchetta@unimi.it

<sup>c</sup>Istituto di Fotonica e Nanotecnologie (IFN), Consiglio Nazionale delle Ricerche (CNR), 20133 Milano, Italy

<sup>d</sup>Dipartimento di Fisica, Politecnico di Milano, 20133 Milano, Italy

<sup>e</sup>CRC Materiali Polimerici (LaMPo), Dipartimento di Chimica, Università di Milano, 20133 Milano, Italy

<sup>\*</sup>Currently at Optoelectronics Research Centre, University of Southampton, Southampton, Hampshire, SO17 1BJ, UK

<sup>†</sup> Electronic Supplementary Information (ESI) available: [details of any supplementary information available should be included here]. See DOI: 10.1039/cXsm00000x/

fractive index  $n = 1.57$  at  $1070$  nm) to study the rheological properties of the three low concentration samples (Aqua 0.25%, Aqua 0.375% and Aqua 0.425%). However, the maximum stress achievable using PS microbeads with our system was not high enough to investigate the fluidized region for Aqua samples at higher concentrations. Therefore, in order to increase the value of the achievable optical stress, we took advantage of the higher refractive index of glass microbeads with a large percentage of Titanium Oxide and Barium Oxide (TBG) (Cospheric BTGMS-4.15 5-22 $\mu\text{m}$ , polydisperse in radius, refractive index  $n = 1.9$  at  $589$  nm). Initially, we experimentally measured the refractive index of the TBG microbeads at the wavelength used in the microrheology experiments, i.e.  $1070$  nm, by performing oscillatory microrheological experiments in fluids of known viscosity (water and glycerol). By sinusoidally modulating the power emitted by the two facing waveguides, it is possible to apply a sinusoidal stress to a trapped microbead, as we extensively reported in a previous work<sup>3</sup>. Assuming that the measurements are carried out in the linear regime of the material, the resulting strain, as measured by the bead displacement, will be also characterized by a sinusoidal function. The material properties can be naturally expressed in terms of the so-called complex compliance  $J^*$ , which is given by:

$$J^* = J' - i \cdot J'' = \frac{\gamma_0}{\sigma_0} (\cos(\delta) - i \cdot \sin(\delta)) \quad (\text{S4})$$

where the term  $J'$  is called storage compliance and accounts for the elastic part while the term  $J''$  is the loss compliance and accounts for the viscous contribution. In Eq. S4,  $\gamma_0 = \Delta x / (2R)$  is the strain amplitude, with  $\Delta x$  being the amplitude of the bead displacement,  $\sigma_0 = F_o / (12\pi R^2)$  is the stress amplitude and  $\delta$  is the so-called loss angle. In the case of a purely viscous fluid, the complex compliance reduces to its imaginary part  $J'' = 1 / (\omega\eta)$ , where  $\omega$  is the oscillation frequency. By considering small microbead oscillations (in the order of few  $\mu\text{m}$ ) around the microchannel center, it is possible to write the following expression:

$$\frac{1}{\omega\eta} = \frac{\Delta x \cdot 6\pi R}{AP_L f(x_{center})} \quad (\text{S5})$$

where  $f(x_{center})$  represents the value of the optical force profile at the channel center. In case TBG microbeads are employed to perform oscillatory microrheological experiments in a Newtonian fluid of known viscosity, such as water or glycerol, it is possible to measure the value of  $f(x_{center})$ , as all the other parameters appearing in Eq. S5 are known. Consequently, the refractive index of the bead at the wavelength of the optical radiation ( $1070$  nm) can be derived by comparing the experimentally measured  $f(x_{center})$  with values obtained by means of numerical simulations based on paraxial ray-optics (PRO) approach<sup>1,2</sup>, performed for different microbead refractive indices. In this way, we determined the refractive index of TBG microbeads at  $1070$  nm to be equal to  $1.85 \pm 0.03$ . This value was obtained under the assumption that the microbead oscillation is small enough (around few  $\mu\text{m}$ ) so that the optical force profile can be considered almost constant in the bead displacement range. Fig. S1 reports a comparison of the optical force profiles calculated for a  $5 \mu\text{m}$  radius PS and TBG microbeads (using the measured refractive index  $n = 1.85$ )

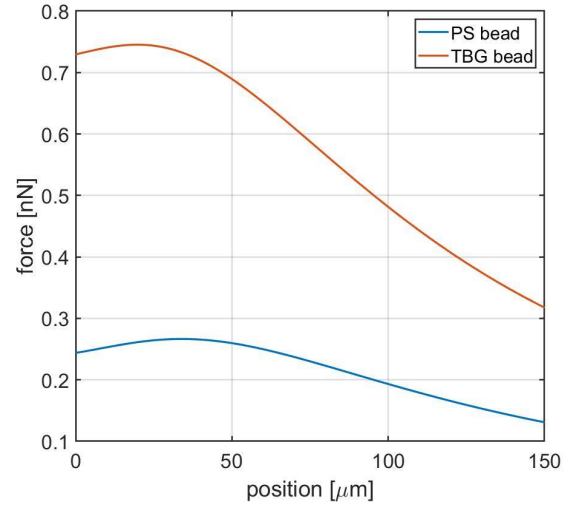


**Fig. S1** Comparison of the optical force profiles for PS ( $n = 1.57$ ) and TBG ( $n = 1.85$ ) microbeads in water, simulated considering an optical power  $P = 1$  W.

in water, considering a value of the optical power equal to  $1$  W emitted by the left waveguide and a beam waist of  $3.8 \mu\text{m}$ . The first observation that can be drawn from the TBG bead curve is that, considering a displacement of  $\pm 5 \mu\text{m}$  around the microchannel center, the relative variation of the optical force profile is less than 4%, confirming the previously made assumption. Moreover, it is worth noticing that the peak value of the optical force profile for the TBG microbead is 2.8 times larger with respect to the one obtained using PS microbeads, at the same power level. Considering, for example, a value of the optical power emitted by the waveguide equal to  $1$  W, we can apply an optical force equal to around  $0.74$  nN on a  $5 \mu\text{m}$  radius TBG microbead, corresponding to a stress of almost  $0.8$  Pa.

### Determination of the linear viscoelastic moduli from optical micro-creep experiments

Because a creep experiment consists of the sudden application of a finite stress value (virtually a step function), it is effectively equivalent to subject the sample to perturbations at various different frequencies, so that we can gain information on its viscoelastic response spectrum, at least in the linear range. At low stresses, we can thus invert creep curves to extract the frequency-dependent linear viscoelastic moduli. To this aim, we used a Fourier-based approach called *i-Rheo*<sup>4</sup>, recently applied to step-stress experiments<sup>5</sup>. In Fig. S2, we compare the resulting storage and loss moduli with bulk small amplitude oscillatory measurements. We found similar values and trend, with a weak frequency dependence, for both the elastic and the viscous components. However, the microscopic estimate is limited to few  $\text{rad/s}$  by small fluctuations in the creep data and by uncertainties in the synchronization between force application and image acquisition.

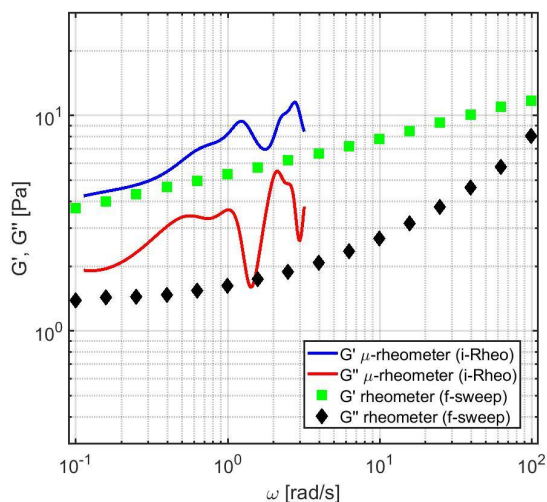


**Fig. S2** Frequency dependence of linear viscoelastic (storage,  $G'$ , and loss,  $G''$ ) moduli in a sample at  $c = 0.375\%$ . Bulk oscillatory measurements (green squares and black diamonds) are compared to *i-Rheo* estimates from a low stress ( $\sigma = 0.15Pa$ ) creep curve (blue and red lines).

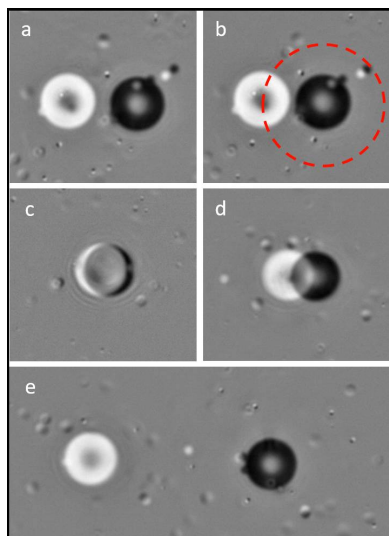


**Fig. S3** Image differences between states of the sample ( $c = 0.375\%$ ) after and before stress application. (a,b) Difference between maximum deformation and the initial state (a) and between the final state after recovery and the initial one (b) for  $\sigma = 0.45Pa$ ; the dashed circle highlights the distance of the farthest permanently displaced tracer. (c-e) Difference between the final and initial states for  $\sigma = 0.25Pa$  (c),  $0.35Pa$  (d) and  $0.6Pa$  (e).

### Imaging experiments

To visualize deformations in the portion of material surrounding the probe, we seeded the microgel samples with small, passive tracers and we took image sequences during creep. Despite the limited spatial and temporal resolution, we can identify the affected region for the maximum deformation and for the unrecovered deformation. To this aim, we take the image difference between the state at 10 seconds after stress application and the initial state (Fig. S3a); and the difference between the state at 10 seconds after stress removal and the initial state (Fig. S3b). In

such images, the grey background corresponds to null difference, i.e. nothing has changed, while white and black pairs correspond to the initial and final states of displaced microbead and tracers, so that the extent, direction and sign of strain can be obtained (as highlighted by red arrows in Fig. 7b-c in the main text). In Fig. S3b, the red dashed circle corresponds to the distance from the microbead center of the farthest tracer permanently displaced after recovery and thus contributes to the estimate of the yielded region. Fig. S3c-e shows similar image differences for the residual deformation at various stress values. The average of at least 3 experiments for each stress is reported in Fig. 7d in units of microbead radius.

### Notes and references

- 1 L. Ferrara, E. Baldini, P. Minzioni, F. Bragheri, C. Liberale, E. D. Fabrizio and I. Cristiani, *Journal of Optics*, 2011, **13**, 75712–75719.
- 2 T. Yang, Y. Chen and P. Minzioni, *Journal of Micromechanics and Microengineering*, 2017, **27**, 123001.
- 3 V. Vitali, G. Nava, G. Zanchetta, F. Bragheri, A. Crespi, R. Oselame, T. Bellini, I. Cristiani and P. Minzioni, *Scientific Reports*, 2020, **10**, 1–11.
- 4 R. M. Evans, M. Tassieri, D. Auhl and T. A. Waigh, *Physical Review E - Statistical, Nonlinear, and Soft Matter Physics*, 2009, **80**, 012501.
- 5 R. Rivas-Barbosa, M. A. Escobedo-Sánchez, M. Tassieri and M. Laurati, *Physical chemistry chemical physics : PCCP*, 2020, **22**, 3839–3848.